Molecular Cancer Therapeutics

EZH2 Inhibition Blocks Multiple Myeloma Cell Growth through Upregulation of Epithelial Tumor Suppressor Genes

Henar Hernando, Kathy A. Gelato, Ralf Lesche, Georg Beckmann, Silke Koehr, Saskia Otto, Patrick Steigemann, and Carlo Stresemann

Abstract

Multiple myeloma is a plasma cell malignancy characterized by marked heterogeneous genomic instability including frequent genetic alterations in epigenetic enzymes. In particular, the histone methyltransferase Enhancer of Zeste Homolog 2 (EZH2) is overexpressed in multiple myeloma. EZH2 is the catalytic component of the polycomb repressive complex 2 (PRC2), a master transcriptional regulator of differentiation. EZH2 catalyzes methylation of lysine 27 on histone H3 and its deregulation in cancer has been reported to contribute to silencing of tumor suppressor genes, resulting in a more undifferentiated state, and thereby contributing to the multiple myeloma phenotype. In this study, we propose the use of EZH2 inhibitors as a new therapeutic approach for the treatment of multiple myeloma. We demonstrate that EZH2 inhibition causes a global reduction of H3K27me3 in multiple myeloma cells, promoting reexpression of EZH2-repressed tumor suppressor genes in a subset of cell lines. As a result of this transcriptional activation, multiple myeloma cells treated with EZH2 inhibitors become more adherent and less proliferative compared with untreated cells. The antitumor efficacy of EZH2 inhibitors is also confirmed *in vivo* in a multiple myeloma xenograft model in mice. Together, our data suggest that EZH2 inhibition may provide a new therapy for multiple myeloma treatment and a promising addition to current treatment options. *Mol Cancer Ther; 15(2); 287–98. ©2015 AACR.*

Introduction

Multiple myeloma is a plasma cell malignancy characterized by abnormal proliferation of clonal plasma cells in the bone marrow, typically accompanied by the secretion of defective monoclonal immunoglobulins (1). Current therapies that have improved the outcome of patients include the proteasome inhibitor bortezomib and immunomodulatory drugs such as thalidomide and lenalidomide (2). Nevertheless multiple myeloma remains an incurable disease with a high rate of relapse and development of drug resistance, and a median survival of less than 5 years (3). The bone marrow microenvironment plays a pivotal role in multiple myeloma proliferation, survival, migration, and resistance to drugs, protecting cells from the cytotoxic effects of chemotherapy and radiation treatment (4). The genetic and epigenetic heterogeneity in multiple myeloma also contributes to relapse, and accordingly finding a druggable oncogenic process common in all patients has not yet been achieved (5).

One of the common genetic alterations in multiple myeloma is the overexpression of the histone methyltransferase enhancer of zeste homolog 2 (EZH2; ref. 6). EZH2 is, along with its paralogue EZH1, the catalytic subunit of Polycomb repressive complex 2 (PRC2), and is responsible for the methylation of histone H3 lysine 27 (H3K27; ref. 7). Methylation of H3K27 is associated with transcriptional repression, and it plays a critical role in regulating genes that determine the balance between cell differentiation and proliferation.

Normal bone marrow plasma cells do not express EZH2; however, gene expression is induced and correlates with tumor burden during progression of multiple myeloma (6). While EZH2 controls H3K27 methylation in multiple myeloma cells, inactivating mutations and deletions of the H3K27 demethylase lysine (K)-specific demethylase 6A (KDM6A, UTX) are frequent in multiple myeloma (8), further contributing to H3K27 aberrant hypermethylation of genes. Enzymes controlling methylation on histone H3 lysine 36 (H3K36), such as histone methyltransferase multiple myeloma SET domain (MMSET), can additionally regulate H3K27 methylation levels and distribution across the genome in multiple myeloma (9). In cells with high levels of MMSET, EZH2 is unable to bind and methylate sites with increased H3K36me2, and is relocated to loci that maintain H3K27 methylation (10). Around 20% of multiple myeloma cases have MMSET overexpression due to the genomic translocation t(4;14) (11), placing the *MMSET* gene under the regulation of strong immunoglobulin enhancers, leading to abnormally high levels of H3K36me2 (12) and a concomitant reduction in H3K27 trimethylation (H3K27me3; ref. 13). Thus, overexpression of MMSET results in a shift of EZH2 function with a reduction of global levels of H3K27me3 and a localized gene-specific increase of H3K27me3. Taken together, frequent genetic alterations of EZH2, UTX and MMSET disrupt the global and/or gene-specific balance of H3K27 methylation in multiple myeloma.

Changes in the H3K27 methylation pathway have emerged as a recurrent phenomenon in many types of cancer, demonstrating that either excess or lack of H3K27 methylation can

Global Drug Discovery, Bayer Pharma AG, Berlin, Germany.

Note: Supplementary data for this article are available at Molecular Cancer Therapeutics Online (http://mct.aacrjournals.org/).

Corresponding Author: Carlo Stresemann, Global Drug Discovery, Bayer Pharma AG, Müllerstr. 178, Berlin 13353, Germany. Phone: 4930-4681-2866; Fax: 4930-4689-93435; E-mail: carlo.stresemann@bayer.com

doi: 10.1158/1535-7163.MCT-15-0486

have oncogenic effects in different indications (14). In multiple myeloma, it has been shown that PRC2 target genes are most often found silenced in myeloma (15). Exploration of EZH2 inhibitors in multiple myeloma models is therefore an attractive field of research which may lead to a broader understanding of multiple myeloma biology and will guide the development of new targeted therapies.

Intensive efforts devoted to developing therapeutic approaches to target EZH2 function led to the discovery of small molecules that specifically inhibit EZH2. First molecules that directly target EZH2 and compete with the cofactor S-adenosylmethionin (SAM) binding have been described. The inhibitor E7438 has shown efficacy in SMARCB1-mutant Rhabdoid tumors (16) and as well as GSK126 and other reported EZH2 inhibitors (17, 18), in EZH2-mutant non-Hodgkin lymphoma (19) where activating mutations are described (20). In addition, effects of EZH2 inhibitors in melanoma (21), ovarian tumors (22), cervical cancer (23), and mixed lineage leukemia (MLL; refs. 24, 25) have been reported. Three first-generation EZH2 inhibitors have recently entered phase I clinical trials (26). In this study, we propose that EZH2 plays an important role in multiple myeloma development and progression. EZH2 inhibition promotes an antiproliferative effect on a subset of multiple myeloma cells, and we provide one possible mechanism by which EZH2 inhibition achieves cell growth inhibition in a cell line panel of various multiple myeloma models.

Materials and Methods

Cell culture

Cell lines NCI-H929, MM.1S, and U-266 were obtained from the ATCC between 2009 and 2014. OPM-2, MOLP-8, LP-1, KMS-12-PE, L-363, and RPMI-8226 were obtained from the Deutsche Sammlung von Mikroorganismen und Zellkulturen (DSMZ) between 2012 and 2013. KMS-11, KMS-28BM, KMS-20, and KMS-34 were obtained from the Japanese Collection of Research Bioresources Cell Bank (JCRB) between 2012 and 2014. Cell lines were authenticated by short tandem repeat (STR) DNA typing at the DSMZ. They were maintained in the recommended cell culture media at 37°C in 5% CO_2.

Antibodies and materials

Primary antibodies used in this study: H3K27me3, H3K36me2, EZH2 (Cell Signaling Technology #9733, #2901, #5246), total histone H3, MMSET, JMJD3, anti-phosphoS5 RNA Pol II (Abcam ab10799, ab75359, ab154985, ab5408), UTX (Bethyl Laboratories A302-374A), E-Cadherin (BD Biosciences 610182), EMP1 (Santa Cruz Biotechnology sc-55717), and GAPDH (Advanced Immunochemical #RGM2). Secondary antibodies used: goat anti-mouse/rabbit IRDye 800 CW (LI-COR Biosciences), Alexa Fluor 680 goat anti-mouse/rabbit IgG, and rabbit anti-goat IgG, anti-rabbit Alexa Fluor 680, anti-mouse Alexa 488 (Life Technologies), and SULFO-TAG anti-rabbit/mouse (Meso Scale Discovery). E7438, CPI169, GSK126, and GSK343 were synthesized in-house.

Proliferation assays

Cells (in triplicate) were treated with dilution series of E7438 from 16 to 0.125 μmol/L, or with DMSO and were incubated for 3 and 7 days. Proliferation was quantified using AlamarBlue (Thermo Fisher Scientific) and fluorescence signal was detected with a VICTOR X3 Multilabel Plate Reader.

Western blot analysis

Cells were lysed in RIPA buffer with Benzonase and protease inhibitors (Roche Diagnostics). Proteins were separated on SDS-PAGE gels and blotted onto nitrocellulose membranes. Experiments were performed in triplicate. Bands were detected and quantified with LI-COR Odyssey Fc Software.

ELISA

Histones were extracted using the EpiXtract Total Histone Extraction Kit (Enzo) and added to 96-well ELISA Standard Plates (Meso Scale Discovery) in triplicate. After overnight incubation, plates were blocked with Blocker A Kit and incubated with the respective antibodies. Read Buffer T 4x was added prior to the measurement in SECTOR Imager 6000 (Meso Scale Discovery).

Gene expression analysis

Cells (2×10^5 per well) were seeded into six-well culture plates 24 hours before treatment. Five replicate wells were then exposed to 2 μmol/L of E7438 or DMSO for 3 days. RNA was extracted using RNeasy Kit (Qiagen). For each sample, 250 ng of total RNA was amplified using the Affymetrix GeneChip WT PLUS Reagent Kit according to the protocol described in User Manual Target Preparation for GeneChip Whole Transcript (WT) Expression Arrays (P/N 703174 Rev. 2). An Affymetrix Human Gene 2.1 ST 96-array plate was hybridized with 3 μg of fragmented and labeled ss cDNA, washed, stained, and scanned according to the protocol described in the User Manual GeneTitan Instrument User Guide for Expression Arrays Plates (P/N 702933 Rev.1) and Affymetrix GeneChip Command Console User's Guide (P/N 702569 Rev.9) using the Affymetrix GeneTitan instrument. These data are available in the ArrayExpress database (www.ebi.ac.uk/arrayexpress) under accession number E-MTAB-3540. Principal component and correlation analyses were used to confirm data reproducibility. Differentially expressed probe sets were determined by carrying out paired *t* test comparisons of treated versus control cells. Significant probe sets with a FDR (Benjamini–Hochberg) < 0.1 were filtered by fold-change > 1.5 using Expressionist-GeneData software. Functional analysis of differentially expressed probe sets was performed using AmiGO Term Enrichment Service for Biological Process (http://amigo.geneontology.org/amigo).

qRT-PCR

RNA (1 μg) was reverse transcribed using SuperScript III First-Strand Synthesis SuperMix (Life Technologies) and cDNA obtained was used for quantifying gene expression in the 7500 Fast Real-Time PCR System (Applied Biosystems) utilizing TaqMan Fast Advanced Master Mix (Life Technologies). Commercial primers used in this study are listed in the Supplementary Materials and Methods.

Chromatin immunoprecipitation

MOLP-8 cells (2×10^6) were treated with 2 μmol/L E7438 or DMSO for 3 days. Standard chromatin immunoprecipitation (ChIP) assays were performed. See Supplementary Materials and Methods for more details.

Cell-cycle distribution by FACS and apoptosis detection

Cells (0.2×10^6 cells/well) were seeded 24 hours before they were treated for 7 days with E7438, at their IC_{50} concentration. DMSO was used as a control. Cells were washed with PBS and

fixed overnight at −20°C with ethanol 70%. Fixed cells were stained with propidium iodide (Sigma P-4170) solution containing RNaseA (Sigma R4875). Fluorescence was measured with FACSCalibur flow cytometer and data were analyzed using BD CellQuest Pro Software. Apoptosis was analyzed using Annexin V-FITC Apoptosis Detection Kit I (BD Biosciences) according to the manufacturer's protocol, fluorescence was measured with FACSCalibur flow cytometer, and data were analyzed using BD CellQuest Pro Software.

Cell imaging

Cells were seeded in CellCarrier-384 Black Optically Clear Bottom plates (PerkinElmer) 24 hours before treatment with 2 μmol/L of E7438 or DMSO, and cultured for 5 days. Transmitted light images were acquired with a 10× magnification with a Molecuar Devices ImageXpress Micro widefield imaging system. Immunofluorescence staining was done with cells attached to Chamber Slides (Thermo Fisher Scientific) treated with Poly-L-Lysine. Cells were fixed with 4% paraformaldehyde, permeabilized with 0.5% Triton X-100 and blocked with 1.0% bovine serum albumin. Staining was done using specific antibodies. DAPI and actin-fluorescent Alexa Fluor 568 (Life Technologies) were used for nuclear and cytoplasmic staining, respectively. Images were acquired with an LSM700 confocal microscope (Zeiss) using 63× magnification.

xCELLigence adhesion quantification

Cells were seeded into 96 wells e-plates (Acea Biosciences) 24 hours before the treatment. Cells (in triplicate) were treated with 2 μmol/L of E7438 and DMSO. Adhesion was monitored by impedance measurement every 15 minutes using the RTCA MP Station (Acea Biosciences).

Multiple myeloma xenograft mouse model

Animal experiments were conducted in accordance with the German animal welfare law, approved by local authorities, and in accordance with the ethical guidelines of Bayer AG. Seven-week-old female scid/scid mice obtained from Charles River Laboratories (Germany) were acclimated for 8 days before tumor cell injection. A total of 1×10^7 MOLP-8 cells were resuspended in 100 μL of 100% Matrigel and injected subcutaneously to the right flank of the mice. Treatment was started at day 4 after tumor inoculation. E7438 or vehicle (PEG400/EtOH 90/10) was administered *per os* twice a day at 250 and 500 mg/kg. Tumor size was measured 2 to 3 times a week for 16 days. For RNA and protein extraction, tumor samples were immediately frozen in liquid nitrogen and stored at −80°C. Frozen tumors were mechanically homogenized using the TissueLyser and Stainless Steel Beads (Qiagen) and RNA and proteins were extracted as described above.

Results

EZH2 inhibition induces time-dependent antiproliferative effects in several multiple myeloma cell lines

A total of 13 multiple myeloma cell lines were selected for the initial set of experiments to characterize EZH2 inhibition effects. Different genetic alterations commonly found in multiple myeloma patients were represented in the selected panel of cell lines (Fig. 1A). Among them were cell lines with and without the t(4;14) translocation, combined with the presence or the absence of UTX protein expression. Although cell lines harboring the t(4;14) translocation all showed elevated mRNA levels of MMSET (Supplementary Fig. S1B), not all cell lines clearly showed this phenotype at the protein level (Fig. 1A and Supplementary Fig. S1A), which might reflect the complexity of possible protein products from the *MMSET* gene (13). However, each of these cell lines presented high amounts of H3K36me2 combined with low levels of H3K27me3, and the inverse occurred for the cell lines without the t(4;14) translocation, confirming results also reported by others (27). The protein levels of EZH2 and JMJD3 (another H3K27me3-specific demethylase not reported to be altered in multiple myeloma) showed slight differences, which did not correlate with global H3K27me3 levels (Fig. 1A).

To determine the effects of EZH2 inhibition on this panel of cell lines, they were treated with increasing concentrations of the E7438 for 3 and 7 days, and cell proliferation was measured (Fig. 1B and Supplementary Fig. S2B). While only in the L-363 cell line a proliferation effect was observed after 3 days of treatment (Supplementary Fig. S2B), after 7 days, more pronounced proliferation effects of at least approximately 50% inhibition were observed in 5 cell lines (KMS-20, KMS-28BM, MOLP-8, RPMI-8226, and U-266). A more pronounced effect of EZH2 inhibition on proliferation on day 7 is expected and can be explained by the mode of action of EZH2 inhibition. H3K27me3 loss precedes the transcriptional activation needed for proliferation defects. We and others have observed that the H3K27me3 mark has slow turnover kinetics (18) and a 2- to 3-day inhibition period is needed for significant demethylation (19, 28).

To investigate the underlying mechanism of proliferation inhibition, effects on the cell cycle were measured after treatment with E7438 for 7 days (Supplementary Fig. S2C). Cell lines were treated with E7438 at the calculated IC_{50} value from proliferation assays, to compare the cycle effects at a similar inhibition level. We observed a general decrease in the percentage of cells in G_2–M accompanied by an increase in sub-G_1 (apoptotic) cells, except for the U-266 cell line which showed only a minor increase in the G_0–G_1 fraction. Similar results for apoptosis induction were obtained by analyzing the Annexin V/propidium iodide–positive cells (Supplementary Fig. S2D). Next, we analyzed the effects of EZH2 inhibition on histone modifications. Global H3K27me3 levels were quantified by Western blot analysis after 3 days of treatment with 0.5 and 2 μmol/L E7438 or DMSO as control. While only a subset of cell lines showed an effect on cell proliferation in response to E7438, H3K27me3 levels were reduced after E7438 treatment in a dose-dependent manner in all tested multiple myeloma cell lines, already at 3 days with 0.5 μmol/L E7438 (Fig. 1C and Supplementary Fig. S2E). To obtain more quantitative data on the effect of E7438, we performed H3K27me3 and H3K36me2 ELISA on extracted histones. Confirming the results observed by Western blot analysis, all cell lines showed reduced levels of H3K27me3 after 3 days of E7438 treatment at 2 μmol/L compared with the DMSO control. In contrast, H3K36me2 levels were not significantly changed after treatment with E7438 (Fig. 1D). It is important to highlight that these experiments were done after 3 days of E7438 treatment, which is a time point with a significant effect on histone methylation which precedes effects on cell proliferation (Fig. 1B and Supplementary Fig. S2B). By comparing the basal levels of these two antagonistic histone modifications in multiple myeloma cell lines, we confirmed interdependency between H3K27me3 and

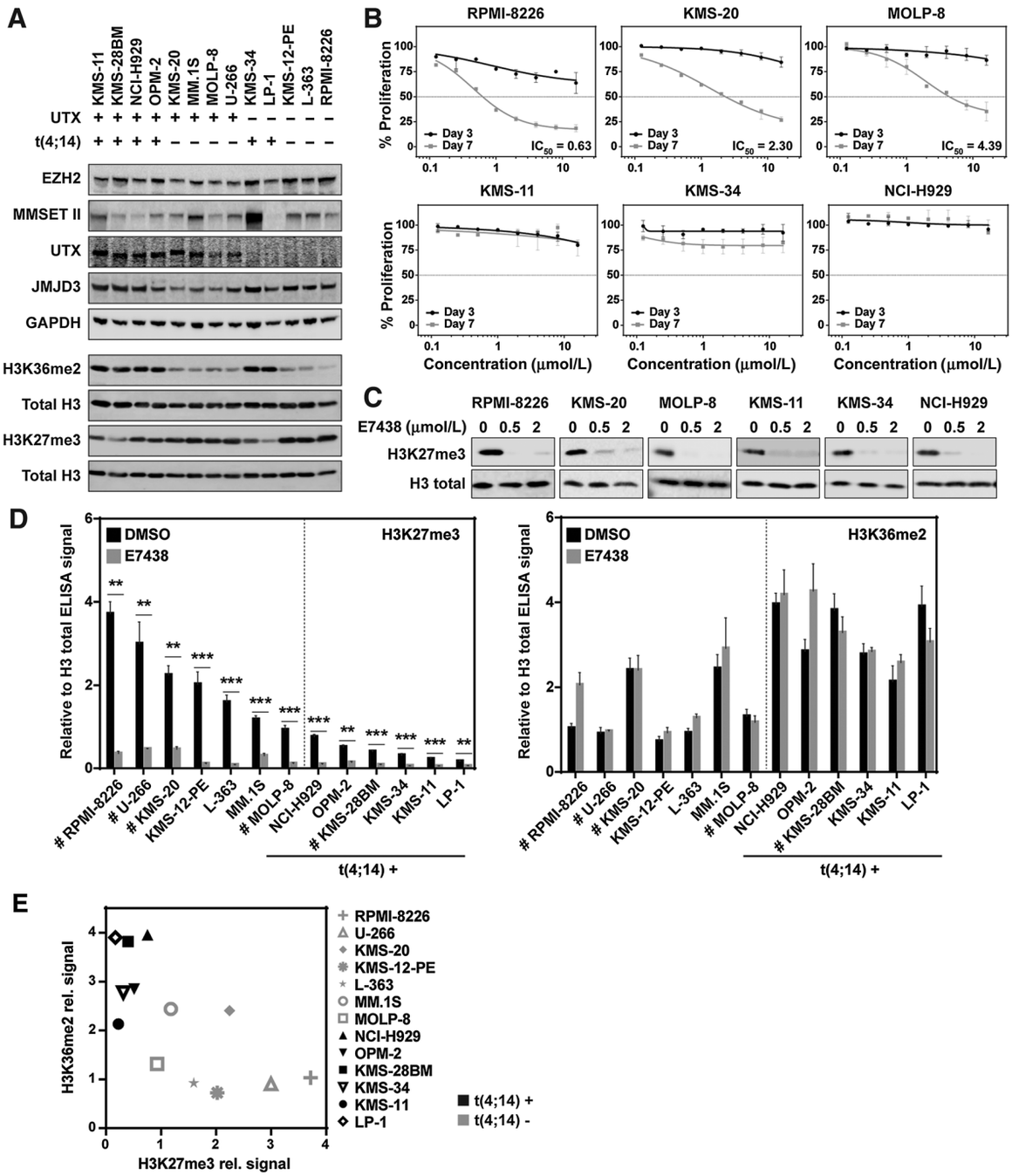

Figure 1.
E7438 treatment inhibits the proliferation of several multiple myeloma cell lines and reduces H3K27me3 levels. A, Western blot analysis of the 13 tested multiple myeloma (MM) cell lines and their different genetic profiles. The primary antibodies used were EZH2 (Cell Signaling Technology #5246), MMSET (Abcam ab75359), UTX (Bethyl Laboratories A302-374A), JMJD3 (from Abcam ab154985), GAPDH (Advanced Immunochemical #RGM2), H3K36me2 (Cell Signaling Technology #2901), H3K27me3 (Cell Signaling Technology#9733), and total histone H3 (Abcam ab10799). B, dose-dependent effects of E7438 on cell proliferation at day 3 (black) and 7 (gray) of six multiple myeloma cell lines (RPMI-8226, KMS-20, MOLP-8, KMS-11, KMS-34, and NCI-H929). Fluorescence values at days 3 and 7 were expressed as a percentage of the DMSO control value and plotted against compound concentrations. The absolute IC_{50} was calculated by fitting a dose–response curve using GraphPad software. C, Western blot analysis of H3K27me3 (Cell Signaling Technology #9733) in six multiple myeloma cell lines (RPMI-8226, KMS-20, MOLP-8, KMS-11, KMS-34, and NCI-H929) tested after 3 days of treatment with DMSO, or 0.5 and 2 μmol/L E7438. Histone H3 (Abcam ab10799) is included as a loading control. D, ELISA quantification of global levels of H3K27me3 (Cell Signaling Technology #9733; left) and H3K36me2 (Cell Signaling Technology #2901; right) relative to total histone H3 (Abcam ab10799) of multiple myeloma cell lines treated with DMSO (black) or with E7438 2 μmol/L (gray) for 3 days. Cell lines with antiproliferation effects after E7438 treatment were marked with # and t(4;14)–positive cell lines were indicated. *P* values were calculated using *t* test compared with DMSO (**, $P \leq 0.01$; ***, $P \leq 0.001$). E, correlation plot of H3K27me3 and H3K36me2 levels quantified by ELISA, showing distribution of t(4;14) positive (black) and negative (gray) cell lines.

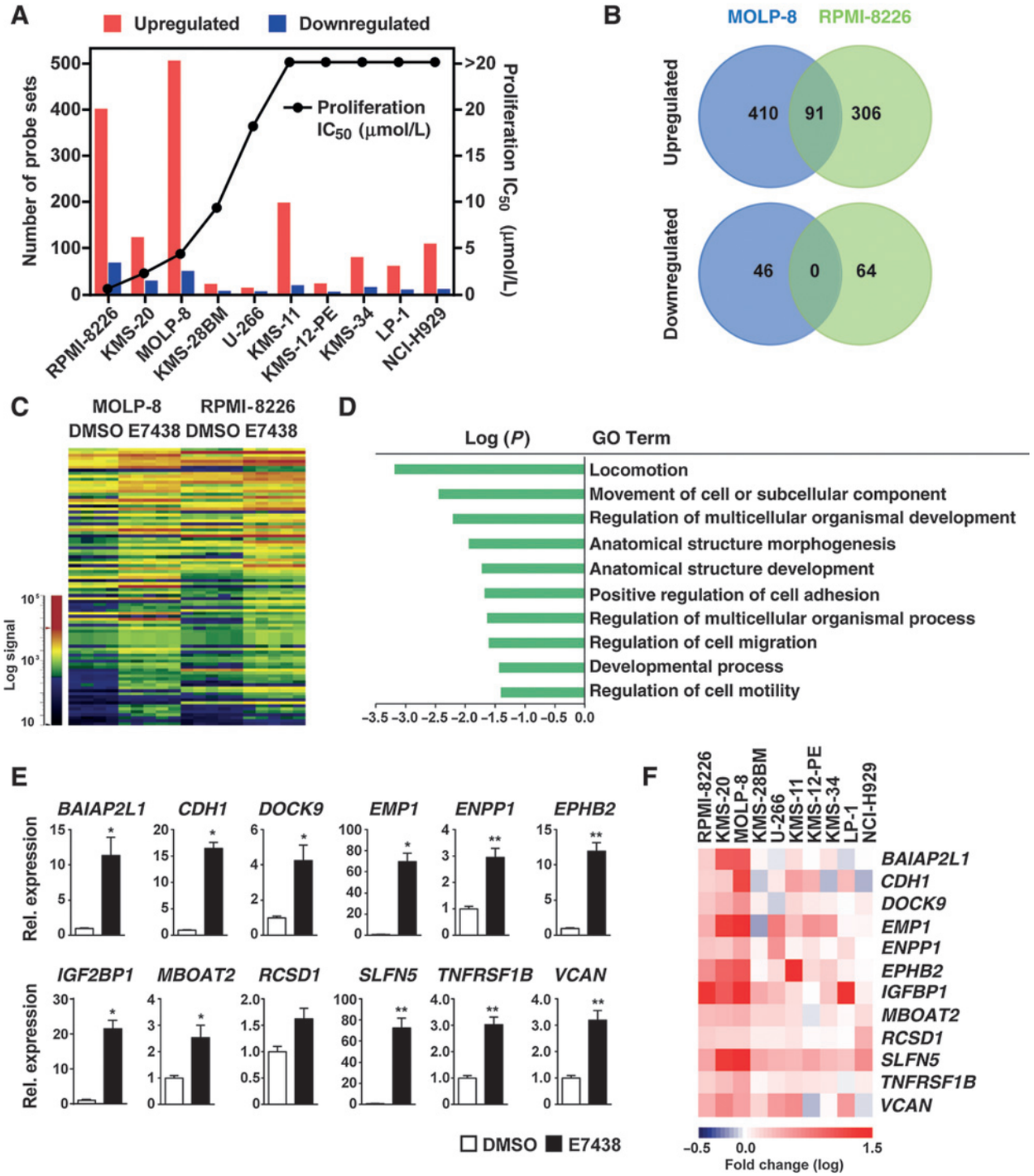

Figure 2.

E7438 treatment promotes transcriptional activation in multiple myeloma (MM) cell lines. A, the number of probe sets showing significantly altered expression [false discovery rate (FDR) < 0.1 and fold change > 1.5] following 72 hours treatment with 2 μmol/L E7438 and its correlation with the IC_{50} in RPMI-8226, KMS-20, MOLP-8, KMS-28BM, U-266, KMS-11, KMS-12-PE, KMS-34, LP-1, and NCI-H929 cell lines. B, Venn diagrams showing the overlap of significantly upregulated and downregulated probes in MOLP-8 and RPMI-8226. C, expression heatmap representing the 93 overlapped probes in MOLP-8 and RPMI-8226 cell lines treated with DMSO or 2 μmol/L E7438. D, AmiGo gene ontology analysis of the 93 overlapped probes in MOLP-8 and RPMI-8226 showing GO categories with a $P < 0.05$. E, qRT-PCR expression levels relative to GAPDH of 12 significantly upregulated genes (from MOLP-8 with FDR < 0.1 and fold change > 1.5) tested in the MOLP-8 cell line. *P* values were calculated using *t* test (*, $P \leq 0.05$; **, $P \leq 0.01$) compared with DMSO. F, heatmap showing expression values for the 12 upregulated genes (from MOLP-8 with FDR < 0.1 and fold change > 1.5) tested in 10 multiple myeloma cell lines. Expression values are represented as log10 fold change of cells treated with 2 μmol/L E7438 relative to cells treated with DMSO.

H3K36me2 based on the underlying genomic alterations. All the cell lines harboring the t(4;14) translocation with an increased expression of the MMSET H3K36 methyltransferase showed a tendency for higher levels of H3K36me2. Elevated levels of H3K36me2 were accompanied by lower H3K27me3 levels, and conversely cells with high H3K27me3 show a tendency to have lower H3K36me2 (Fig. 1E). Interestingly, the three cell lines showing the highest levels of global H3K27me3 responded in the proliferation assay, which might indicate a higher degree of cancer cell addiction towards EZH2 activity. Notably, the presence or absence of UTX did not seem to have an effect on the global H3K27me3 levels.

To reconfirm that H3K27me3 demethylation does not always result in proliferation effects, we also tested three other EZH2 inhibitors (GSK126, GSK343, and CPI169) in KMS-11 (Supplementary Fig. S3A). Notably all inhibitors showed comparable target inhibition with an almost complete reduction in total H3K27me3 methylation with 2 μmol/L after 3 days of treatment (Supplementary Fig. S3B). No proliferation effects were observed in KMS11 for any inhibitor used. GSK126 and GSK343 showed some additional proliferation effects with higher concentrations (>7.5 μmol/L), but which could not be connected to an improved methylation inhibition in comparison with E7438 or CPI169 (Supplementary Fig. S3B). Together, our data reveal that E7438 reduces H3K27me3 levels in all tested multiple myeloma cell lines, without significant changes in H3K36me2, causing a time-dependent antiproliferative response in a subset of multiple myeloma cell lines.

EZH2 inhibition promotes transcriptional activation in multiple myeloma cell lines

Gene expression was analyzed in 10 of the multiple myeloma cell lines, including the cell lines showing antiproliferation effects with E7438 treatment (KMS-20, KMS-28BM, MOLP-8, RPMI-8226, and U-266) and 5 of the nonaffected cell lines (KMS-11, KMS-12-PE, KMS-34, LP-1, and NCI-H929). These data are available in the ArrayExpress database (www.ebi.ac.uk/arrayexpress) under accession number E-MTAB-3540. All cell lines were treated with 2 μmol/L of E7438 or DMSO control for 3 days. E7438 differentially altered the expression in the multiple myeloma cell lines ranging from a few hundreds of gene probes [false discovery rate (FDR) < 0.1 and fold change > 1.5] in MOLP-8 to only minor changes in the U-266 cell line (Fig. 2A). In agreement with the silencing role of EZH2, most of the genes were upregulated upon the global loss of H3K27me3. The number of upregulated probes in each cell line in general correlated only partially with their E7438 IC_{50} values (Fig. 2A). RPMI-8226 and MOLP-8 cell lines showed the most robust transcriptional activation after 3 days, which also translated to lower IC_{50} proliferation inhibition by E7438 after 7 days of treatment. The number of gene probes activated in KMS-20 cells with a proliferative IC_{50} of 2.3 μmol/L was comparable with KMS-11, KMS-34, and NCI-H929 cell lines, which showed no detectable proliferation effects after 7 days of treatment. Surprisingly, KMS-28BM, U-266, and KMS-12-PE showed only minor transcriptional changes even with globally reduced H3K27me3 levels (compare with Supplementary Fig. S2E). Therefore, addiction to the H3K27me3 methylation mark for transcriptional regulation seems to be variable between multiple myeloma cell lines.

In a deeper analysis of all overlapping gene probes significantly changed specifically in RPMI-8226 and MOLP-8, we found 91 probes upregulated in common and no common probes downregulated (Fig. 2B and C). Gene ontology analysis showed enrichment of different pathways (Fig. 2D), a major one being related to cell structure, adhesion, and migration. To characterize further the underlying molecular mechanisms of EZH2 inhibition in multiple myeloma, we focused in the next set of the experiments on the MOLP-8 cell line that had the highest number of significant transcriptional changes. To validate the expression screen results, we selected a subset of 12 upregulated genes for qRT-PCR analysis. Genes were selected from enriched categories of the gene ontology analysis, and were mostly related to cell adhesion. Each gene was confirmed to be upregulated after treatment with E7438 (Fig. 2E). Results were independently confirmed with an additional EZH2 inhibitor, GSK126 (Supplementary Fig. S4A). In addition, we observed that these genes showed a clear tendency for upregulation in all tested cell lines, regardless of their sensitivity to E7438 in the proliferation assay (Fig. 2F) and despite the limited overlap

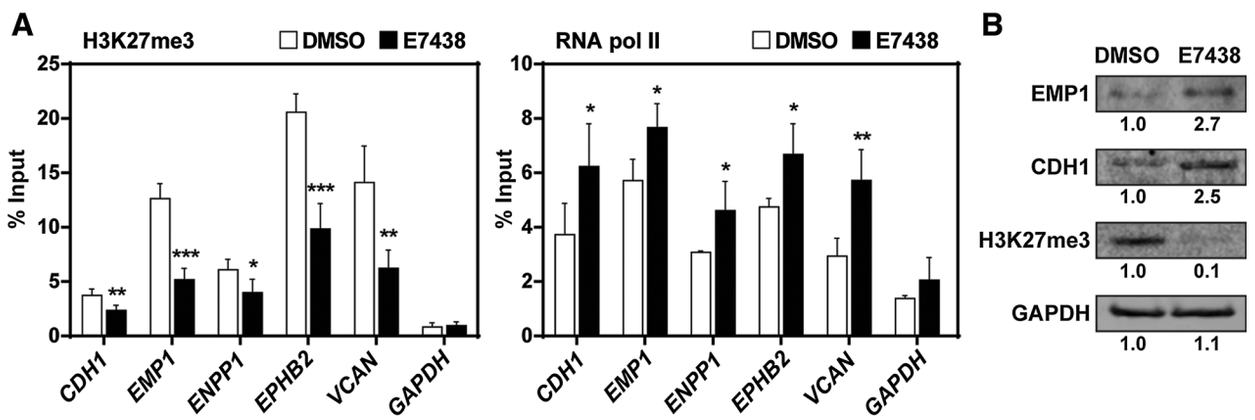

Figure 3.
E7438 treatment induces local reduction of H3K27me3 in promoter regions of upregulated genes. A, H3K27me3 (Cell Signaling Technology #9733; left) and active (phosphorylated) RNA pol II (Abcam ab5408; right) ChIP signal reported as percent of input at *CDH1*, *EMP1*, *ENPP1*, *EPHB2*, and *VCAN* gene promoter regions. *P* values were calculated using *t* test (*, $P \leq 0.05$; **, $P \leq 0.01$; ***, $P \leq 0.001$) compared with DMSO. B, Western blot analysis of E-cadherin (*CDH1*; BD Biosciences 610182), EMP1 (Santa Cruz Biotechnology sc-55717) and H3K27me3 (Cell Signaling Technology #9733), in DMSO and 2 μmol/L E7438 MOLP-8–treated cells. GAPDH (Advanced Immunochemical #RGM2) is used as a loading control. Quantification of Western blot signal was done using Odyssey software.

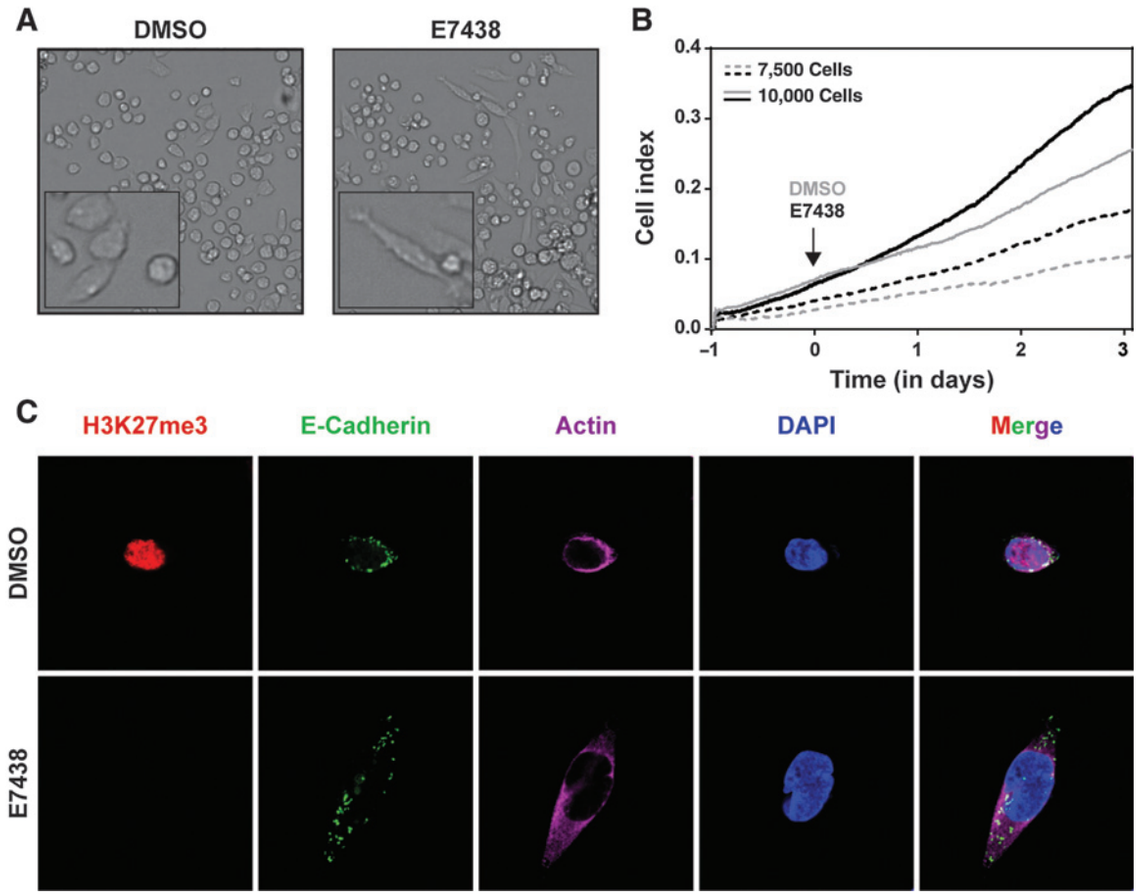

Figure 4.
E7438 treatment increases adhesion of MOLP-8 cells. A, transmitted light pictures of live MOLP-8 cells 5 days after treatment with DMSO control or 2 μmol/L E7438, using a 10× objective. Bottom left square, detail of cells with 1.5× zoom. B, xCelligence adherence measurement showing the cell index of adherent cells treated with DMSO (gray) or 2 μmol/L E7438 (black). Measurements were taken over 4 days using different numbers of starting cells (7,500 and 10,000). C, immunofluorescence staining of H3K27me3 (Cell Signaling Technology #9733; red), E-cadherin (BD Biosciences 610182; green), actin (Life Technologies A12374; magenta), and DAPI (blue) and the merged image, in MOLP-8 cells treated with DMSO or 2 μmol/L E7438 for 5 days.

observed comparing all cell lines (Supplementary Tables S1A and S1B). These results showed significant transcriptional activation after E7438 treatment in multiple myeloma cell lines, revealing that most of the upregulated genes were related with cell structure, adhesion, and migration.

E7438 induces local reduction of H3K27me3 at the promoter region of epithelial tumor suppressor genes

To further explore the regulation of the selected adhesion-related genes by EZH2, we analyzed gene-specific H3K27me3 levels by ChIP and their expression at the protein level. To correlate the expression changes with the local loss of H3K27me3, ChIP experiments were performed. Enrichment of H3, H3K27me3, or phosphorylated RNA Pol II after ChIP was quantified in different regions surrounding the transcription start site (TSS) of *CDH1*, *EMP1*, *VCAN*, *EPHB2*, and *ENPP1* genes, while *GAPDH* served as a control. H3K27me3 occupancy significantly decreased at all analyzed genes after E7438 treatment (Fig. 3A). The basal levels of H3K27me3 before treatment in upregulated genes were high compared with *GAPDH*, indicating that they were potentially EZH2 targets marked by H3K27me3. A decrease of H3K27me3 in the promoter region of these genes after E7438 treatment presumably would allow for an increased binding of RNA Pol II and the initiation of transcription. Accordingly, we detected significant enrichment of RNA Pol II in the promoter region of analyzed genes after treatment (Fig. 3A). These results confirmed the transcriptional activation observed in the gene expression analysis and qRT-PCR. Total histone H3 enrichment after ChIP was comparable among the samples, and the IgG control showed negligible signal, confirming that overall histone H3 content did not lead to the loss of H3K27me3, and that the nonspecific signal was low (Supplementary Figs. S4C and S5). Notably, ChIP results have been re-produced independently with the GSK126 inhibitor (Supplementary Fig. S4B). Western blot experiments demonstrated that the observed upregulation at the transcription level was translated to an increase also at the protein level. We observed more than double the protein levels of E-cadherin (*CDH1* gene) and EMP1, two key adherence-related proteins, in MOLP-8 cells treated with E7438 in comparison with the DMSO control (Fig. 3B). We conclude that global loss of H3K27me3 was also observed at the gene-specific level and led to an increased expression of mRNA and protein.

EZH2 inhibition increases adhesion of multiple myeloma cells by morphologic changes

Most of the upregulated genes from the expression analysis were described as epithelial tumor suppressor genes closely connected to adhesion and a more epithelial phenotype (29). Therefore, we speculated that their reexpression could increase adherence properties in multiple myeloma cells. We closely analyzed MOLP-8 cell adhesion and morphology after E7438 treatment. This multiple myeloma cell line originally consisted of a mixture of predominantly suspension cells with some slightly adherent cells (30). However, after treatment with 2 μmol/L E7438, the number of adherent cells increased and their morphology changed, with many cells becoming elongated rather than round (Fig. 4A). To quantify the increase in the MOLP-8 adherent population after treatment with E7438, we used xCelligence technology. An increase in signal indicates an increase in number of live adherent cells. Even though E7438 induces a proliferation arrest in MOLP-8 cells (Fig. 1B), an elevated number of adherent cells in MOLP-8 was detected (Fig. 4B). We obtained similar results using GSK126 (Supplementary Fig. S4D). To further investigate the phenotype, the protein expression of the epithelial tumor suppressor gene E-cadherin, H3K27me3, and actin distribution was analyzed *in situ* (Fig. 4C). In treated cells, characterized by the absence of H3K27me3, a larger fraction of cells showed a more elongated morphology with cell–cell junctions. E-cadherin was localized mostly in trafficking vesicles. Untreated MOLP-8 cells were more rounded, isolated, and with the E-cadherin signal surrounding the nuclei (Fig. 4C). Altogether, treatment with an EZH2 inhibitor induced expression of epithelial/adherence–associated genes in MOLP-8 cells and modulated their morphology to a more spindle-like and adherent phenotype.

EZH2 inhibition shows significant antitumor efficacy *in vivo*

The multiple myeloma xenograft model MOLP-8 was used to evaluate whether the observed changes in cell morphology and gene expression translate to antitumor efficacy *in vivo*. Therefore, three groups of tumor bearing mice were treated *per os*, twice daily with the following treatments. The first group was treated with vehicle (PEG400/EtOH 90/10) only (control group), the second group was treated with E7438 at 500 mg/kg, *per os*, twice daily, and the third group with 250 mg/kg *per os*, twice daily. Tumors of mice treated with E7438 (500 mg/kg, BID, *per os*) showed a significantly slower tumor progression based on tumor volume (Fig. 5A) and tumor weight (Fig. 5B) compared with the vehicle control group, with no effect on mouse body weight (Supplementary Fig. S6). In addition, levels of H3K27me3 were measured within the tumor tissue. Western blot analysis showed reduced levels of H3K27me3 in both treated groups at 250 and 500 mg/kg (Fig. 6A). Quantitative detection by ELISA showed that levels of H3K27me3 in the 500 mg/kg treated mice were significantly lower compared with mice treated at 250 mg/kg (Fig. 6B). Furthermore, we analyzed the target genes identified in our *in vitro* studies in the tumor tissues *ex vivo*. All target genes were significantly upregulated in tumors from mice treated at 500 mg/kg compared with control. Mice treated with 250 mg/kg inhibitor showed only partial upregulation relative to the control (Fig. 6C and D). Together with the methylation data (Fig. 6B), we conclude that 250 mg/kg treatment did not fully inhibit EZH2-mediated gene repression, which is necessary to inhibit *in vivo* tumor growth in the MOLP-8 model. In summary, these data confirm that the *in vitro* observed antiproliferation efficacy and induction of tumor-suppressive genes after EZH2 inhibition translated to reduced tumor xenograft growth *in vivo*. In both systems, E7438 caused H3K27me3 reduction accompanied by upregulation of EZH2 target genes.

Discussion

Multiple myeloma is a plasma cell malignancy for which there is no pharmacologic treatment that leads to a cure (3). Therefore, establishment of new therapies for this disease could be a valuable addition to current treatment options (31). Multiple myeloma is characterized by widespread dissemination of the bone marrow with multiple focal lesions which requires the disruption of cell-adhesive functions to invade new regions through systemic recirculation (32). Alterations in histone-modifying enzymes like

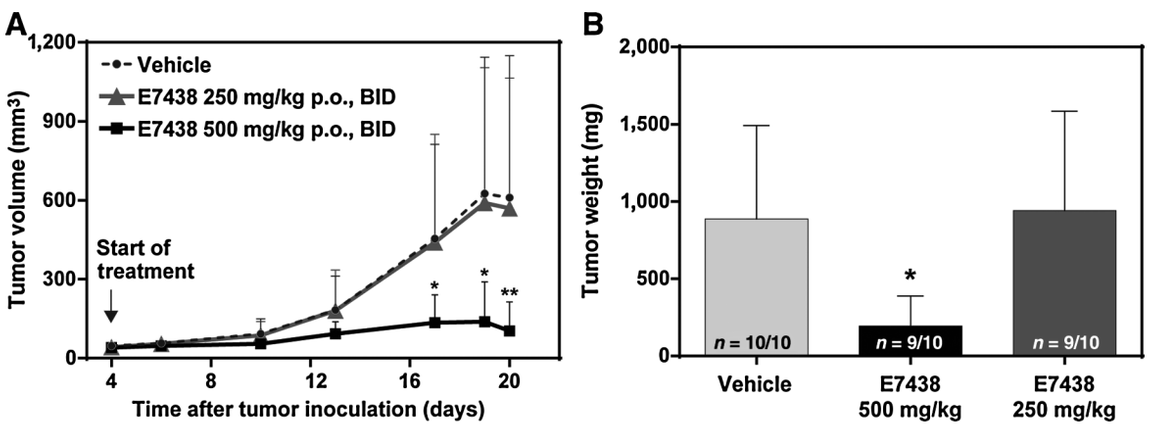

Figure 5.
In vivo inhibition of tumor growth with E7438. A, effect of E7438 on tumor volume of MOLP-8 xenograft mice treated with vehicle, 250 mg/kg or 500 mg/kg of E7438 *per os* (p.o.) twice daily (BID) for 16 days after tumor inoculation. *, $P \leq 0.05$; **, $P \leq 0.01$, significant differences compared with vehicle using ANOVA, Holm–Sidak method (based on log data). B, effect of E7438 on tumor weight in mice treated with vehicle, 250 mg/kg and 500 mg/kg of E7438 *per os* twice daily for 16 days after tumor inoculation. *, $P \leq 0.05$ significant difference compared with vehicle using ANOVA, Holm–Sidak method (based on log data).

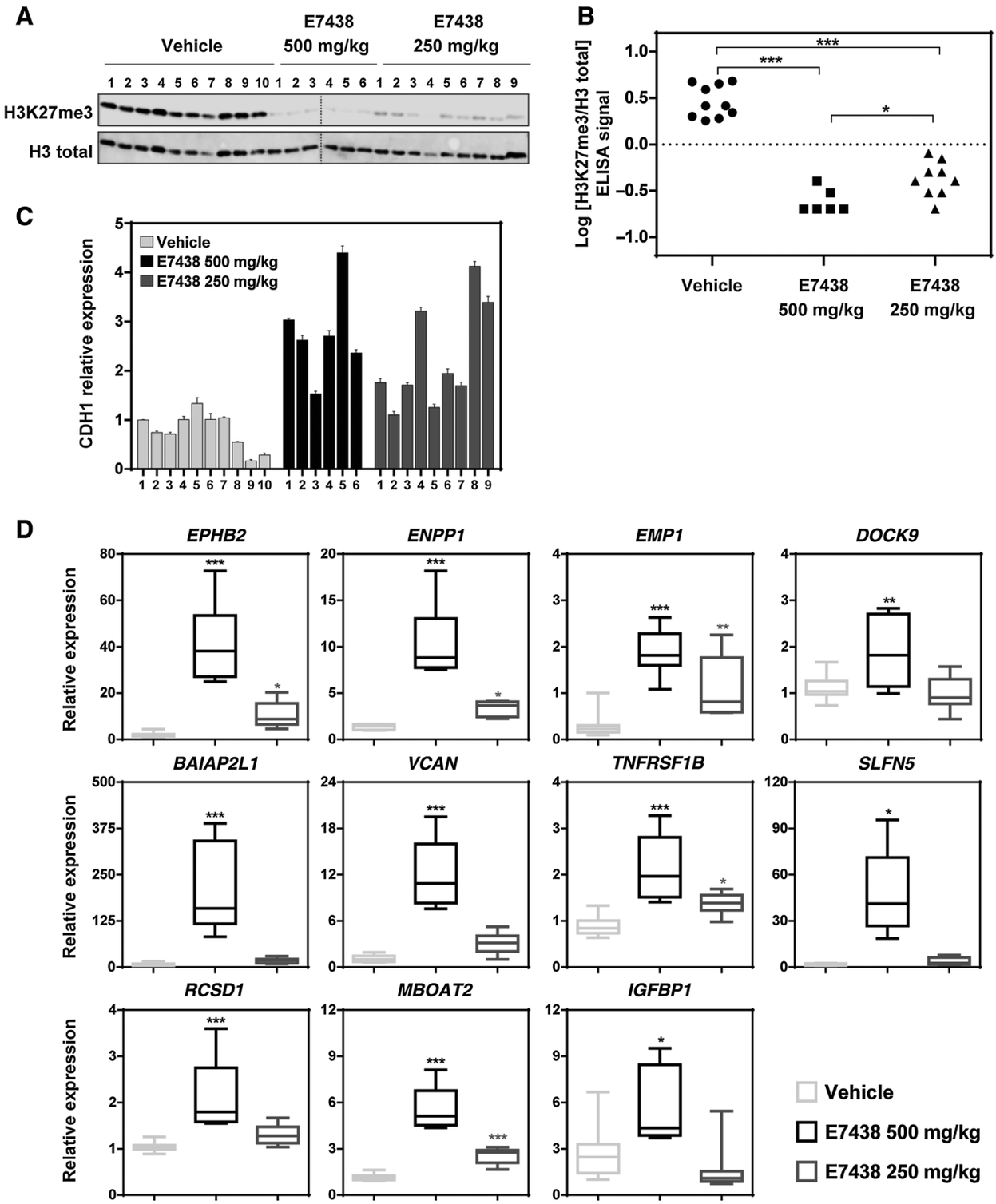

Figure 6.

In vivo reduction of H3K27me3 and activation of transcription with E7438. A, Western blot analysis of H3K27me3 (Cell Signaling Technology #9733) in tumors from MOLP-8 xenograft mice treated with vehicle, 250 mg/kg or 500 mg/kg of E7438. Histone H3 (Abcam ab10799) levels were used as a loading control. B, ELISA quantification of H3K27me3 (Cell Signaling Technology #9733) levels relative to total histone H3 (Abcam ab10799) levels in mice treated with vehicle, 500 mg/kg or 250 mg/kg of E7438. *P* values were calculated using the *t* test to compare each group with the others (*, $P \leq 0.05$; ***, $P \leq 0.001$). C, qRT-PCR expression levels of CDH1 in each tumor sample from mice belonging to vehicle, 250 mg/kg, or 500 mg/kg of treatment groups. D, qRT-PCR expression levels relative to GAPDH of 11 upregulated genes (from MOLP-8 with FDR < 0.1 and fold change > 1.5). Box plots represent the mean, minimum, and maximum value for the expression for each vehicle (light gray), 500 mg/kg (black), and 250 mg/kg (dark gray) treatment groups. *P* values were calculated using ANOVA compared with vehicle (*, $P \leq 0.05$; **, $P \leq 0.01$ and ***, $P \leq 0.001$).

EZH2/UTX/MMSET have been frequently observed and point towards a potential driving role of epigenetic reprogramming of multiple myeloma (33). We uncovered an antiproliferative activity of EZH2 inhibition *in vitro* in a set of multiple myeloma cell lines and translated these findings to an *in vivo* xenograft model. Treatment with an EZH2 inhibitor resulted in upregulation of gene expression, which generally correlates with the role of EZH2 as a transcriptional repressor (34). MOLP-8 and RPMI-8226 cell line models showed the most significant upregulation of genes, which also translated to robust inhibition of proliferation. But expression changes (with the threshold levels and assay conditions employed in our study) did generally not completely correlate with proliferation effects (Fig. 2A). This observation is different from reports in lymphoma cell lines where a direct correlation between expression profiles and the IC_{50} in proliferation assays has been observed for GSK126 (20). This difference indicates a complex underlying genetic diversity in multiple myeloma model systems. Different genetic and epigenetic drivers are potentially necessary to drive malignant transformation and are needed for cell proliferation.

For the H3K27 methylation/PRC2 pathway, several different gene mutations leading to elevated levels of methylation and gene repression have been proposed to predict a potential addiction to EZH2 activity in cancers (14, 35, 36). Particularly in multiple myeloma, several alterations have been proposed to be directly correlated with sensitivity to EZH2 inhibition. MMSET overexpression and UTX loss-of-function mutations have been proposed in previous studies (8, 9), to lead to aberrant H3K27 methylation and transcriptional repression in multiple myeloma. However, in our study, we did not find a clear correlation of EZH2 inhibitor sensitivity with a distinct genetic mutational profile. Only the RPMI-8226 cell line from the five UTX-mutated cell lines showed a significant response in gene expression and proliferation. In the t(4;14)–positive cell lines we could confirm reports of globally increased levels of H3K36 methylation and decreased levels of H3K27 methylation (13). Despite significant gene upregulation in some of the t(4;14) positive cell lines after treatment with E7438 only KMS-28BM showed a proliferation response. A potential limitation of our proliferation results could be the experimental assay system used. Three-dimensional cultures approximating physiologic conditions have been proposed for EZH2 inhibitors to fully cover potential effects of epigenetic reprogramming (21, 37). Nevertheless, our gene expression profiling after loss of global H3K27me3 is different for cell lines having comparable genetic alterations. Therefore, genetic alterations predicting sensitivity to EZH2 inhibition remain elusive and further studies are needed.

We describe for the first time, to our knowledge, a potential role for EZH2 in the regulation of adherence and epithelial–mesenchymal differentiation genes in multiple myeloma. EZH2 has been generally proposed to be critical for the regulation of epithelial–mesenchymal transition (EMT)-associated master genes in cancer (38, 39). We identified several genes involved in adherence, which showed a general trend for upregulation in all analyzed models (see Fig. 2F). Our data, together with recent publications in additional indications such as melanoma (21), breast cancer (40), renal cell carcinoma (41), cervical cancer (23), and oral squamous carcinoma (42) further indicates regulation of EMT and/or ECM (extracellular matrix) adhesion signaling as a fundamental feature of EZH2-mediated malignant reprogramming in cancer.

Multiple myeloma is characterized by widespread dissemination of the bone marrow at diagnosis, with multiple focal lesions in the bone marrow, recirculation into the peripheral blood, and reentrance or homing of multiple myeloma cells into new sites promoting metastasis (32). Our study suggests that EZH2 might play an important role in shaping the interactions between multiple myeloma cells and the microenvironment, regulating their adherence and their capacity to migrate. That EZH2 inhibition promotes adherence properties in multiple myeloma cells could be beneficial, because it might prevent multiple myeloma cell dissemination and new colonization within the bone marrow, thus abrogating metastasis. One of the most important drivers in EMT is the downregulation of E-cadherin, which has been observed to be directly repressed by EZH2 in cancer (39). The E-cadherin gene, *CDH1*, is upregulated in almost all the cell lines tested in this study, independent of their response to treatment. During EMT, cells lose polarity and cell–cell adhesion and gain migratory and invasive properties. Some examples uncovered in our study regulating similar processes are *EMP1* (epithelial membrane protein 1). Reduced levels of EMP1 were associated with tumor invasion, lymph node metastasis, clinical stage, and cell differentiation (43–45). EMP1 is an integral tetraspan membrane protein whose function has been recently described to be involved in epithelial tight junction formation. *EPHB2* is a receptor tyrosine kinase from the ephrin family which is involved in multiple critical aspects of cell adhesion and migration and a putative tumor suppressor (46, 47). Another example is *DOCK9* (dedicator of cytokinesis 9), which belongs to the Dock family of evolutionarily conserved exchange factors for the Rho GTPases Rac and Cdc42, regulating actin cytoskeleton, cell adhesion, and migration (48). SLFN5, a protein, was described to have a key role in controlling motility and invasiveness of renal cell carcinoma and melanoma cells (49, 50). SLFN5 negatively controls expression of matrix metalloproteinases (*MMP*), and several other genes involved in the control of malignant cell motility. Multiple myeloma results from a combination of multiple genetic and epigenetic factors, leading to the development and progression of the disease. The relative complexity of multiple myeloma prevents straightforward mutation-based or other correlative measures to predict proliferation responses towards EZH2 and other inhibitors. Nevertheless, we demonstrated a role of EZH2 in multiple myeloma survival and as regulator of differentiation processes controlling adhesion and migration. Therefore, further exploration of EZH2 inhibitors for multiple myeloma treatment is strongly supported, having the potential to be a promising addition to the current treatments used for multiple myeloma patients.

Disclosure of Potential Conflicts of Interest

R. Lesche reports receiving a commercial research grant from and having ownership interest (including patents) in BAYER AG. No potential conflicts of interest were disclosed by the other authors.

Disclaimer

All authors are employees of Bayer Pharma AG, and the research work was conducted under the employment of Bayer Pharma AG.

Authors' Contributions

Conception and design: H. Hernando, C. Stresemann
Development of methodology: H. Hernando, K.A. Gelato
Acquisition of data (provided animals, acquired and managed patients, provided facilities, etc.): K.A. Gelato, R. Lesche, S. Koehr, S. Otto, P. Steigemann

Analysis and interpretation of data (e.g., statistical analysis, biostatistics, computational analysis): H. Hernando, K.A. Gelato, R. Lesche, G. Beckmann, S. Koehr, C. Stresemann
Writing, review, and/or revision of the manuscript: H. Hernando, K.A. Gelato, R. Lesche, G. Beckmann, S. Koehr, C. Stresemann
Administrative, technical, or material support (i.e., reporting or organizing data, constructing databases): R. Lesche
Study supervision: C. Stresemann

The costs of publication of this article were defrayed in part by the payment of page charges. This article must therefore be hereby marked *advertisement* in accordance with 18 U.S.C. Section 1734 solely to indicate this fact.

Received June 10, 2015; revised October 14, 2015; accepted November 9, 2015; published OnlineFirst November 20, 2015.

References

1. Rollig C, Knop S, Bornhauser M. Multiple myeloma. Lancet 2015;385: 2197–208.
2. Mahindra A, Laubach J, Raje N, Munshi N, Richardson PG, Anderson K. Latest advances and current challenges in the treatment of multiple myeloma. Nat Rev Clin Oncol 2012;9:135–43.
3. Joao C, Costa C, Coelho I, Vergueiro MJ, Ferreira M, da Silva MG. Long-term survival in multiple myeloma. Clin Case Rep 2014;2:173–9.
4. Romano A, Conticello C, Cavalli M, Vetro C, La Fauci A, Parrinello NL, et al. Immunological dysregulation in multiple myeloma microenvironment. BioMed Res Int 2014;2014:198539.
5. Abdi J, Chen G, Chang H. Drug resistance in multiple myeloma: latest findings and new concepts on molecular mechanisms. Oncotarget 2013;4: 2186–207.
6. Croonquist PA, Van Ness B. The polycomb group protein enhancer of zeste homolog 2 (EZH 2) is an oncogene that influences myeloma cell growth and the mutant ras phenotype. Oncogene 2005;24:6269–80.
7. Crea F, Fornaro L, Bocci G, Sun L, Farrar WL, Falcone A, et al. EZH2 inhibition: targeting the crossroad of tumor invasion and angiogenesis. Cancer Metastasis Rev 2012;31:753–61.
8. van Haaften G, Dalgliesh GL, Davies H, Chen L, Bignell G, Greenman C, et al. Somatic mutations of the histone H3K27 demethylase gene UTX in human cancer. Nat Genet 2009;41:521–3.
9. Popovic R, Martinez-Garcia E, Giannopoulou EG, Zhang Q, Zhang Q, Ezponda T, et al. Histone methyltransferase MMSET/NSD2 alters EZH2 binding and reprograms the myeloma epigenome through global and focal changes in H3K36 and H3K27 methylation. PLoS Genet 2014;10: e1004566.
10. Yuan W, Xu M, Huang C, Liu N, Chen S, Zhu B. H3K36 methylation antagonizes PRC2-mediated H3K27 methylation. J Biol Chem 2011; 286:7983–9.
11. Keats JJ, Reiman T, Belch AR, Pilarski LM. Ten years and counting: so what do we know about t(4;14)(p16;q32) multiple myeloma. Leuk Lymphoma 2006;47:2289–300.
12. Stec I, Wright TJ, van Ommen GJ, de Boer PA, van Haeringen A, Moorman AF, et al. WHSC1, a 90 kb SET domain-containing gene, expressed in early development and homologous to a Drosophila dysmorphy gene maps in the Wolf-Hirschhorn syndrome critical region and is fused to IgH in t(4;14) multiple myeloma. Hum Mol Genet 1998;7:1071–82.
13. Martinez-Garcia E, Popovic R, Min DJ, Sweet SM, Thomas PM, Zamdborg L, et al. The MMSET histone methyl transferase switches global histone methylation and alters gene expression in t(4;14) multiple myeloma cells. Blood 2011;117:211–20.
14. Ezponda T, Licht JD. Molecular pathways: deregulation of histone h3 lysine 27 methylation in cancer-different paths, same destination. Clin Cancer Res 2014;20:5001–8.
15. Kalushkova A, Fryknas M, Lemaire M, Fristedt C, Agarwal P, Eriksson M, et al. Polycomb target genes are silenced in multiple myeloma. PLoS ONE 2010;5:e11483.
16. Knutson SK, Warholic NM, Wigle TJ, Klaus CR, Allain CJ, Raimondi A, et al. Durable tumor regression in genetically altered malignant rhabdoid tumors by inhibition of methyltransferase EZH2. Proc Natl Acad Sci U S A 2013;110:7922–7.
17. Qi W, Chan H, Teng L, Li L, Chuai S, Zhang R, et al. Selective inhibition of Ezh2 by a small molecule inhibitor blocks tumor cells proliferation. Proc Natl Acad Sci U S A 2012;109:21360–5.
18. Bradley WD, Arora S, Busby J, Balasubramanian S, Gehling VS, Nasveschuk CG, et al. EZH2 inhibitor efficacy in non-Hodgkin's lymphoma does not require suppression of H3K27 monomethylation. Chem Biol 2014;21: 1463–75.
19. Knutson SK, Kawano S, Minoshima Y, Warholic NM, Huang KC, Xiao Y, et al. Selective inhibition of EZH2 by EPZ-6438 leads to potent antitumor activity in EZH2-mutant non-Hodgkin lymphoma. Mol Cancer Ther 2014;13:842–54.
20. McCabe MT, Ott HM, Ganji G, Korenchuk S, Thompson C, Van Aller GS, et al. EZH2 inhibition as a therapeutic strategy for lymphoma with EZH2-activating mutations. Nature 2012;492:108–12.
21. Barsotti AM, Ryskin M, Zhong W, Zhang WG, Giannakou A, Loreth C, et al. Epigenetic reprogramming by tumor-derived EZH2 gain-of-function mutations promotes aggressive 3D cell morphologies and enhances melanoma tumor growth. Oncotarget 2015;6:2928–38.
22. Bitler BG, Aird KM, Garipov A, Li H, Amatangelo M, Kossenkov AV, et al. Synthetic lethality by targeting EZH2 methyltransferase activity in ARID1A-mutated cancers. Nat Med 2015;21:231–8.
23. Ding M, Zhang H, Li Z, Wang C, Chen J, Shi L, et al. The polycomb group protein enhancer of zeste 2 is a novel therapeutic target for cervical cancer. Clin Exp Pharmacol Physiol 2015;42:458–64.
24. Konze KD, Ma A, Li F, Barsyte-Lovejoy D, Parton T, Macnevin CJ, et al. An orally bioavailable chemical probe of the Lysine Methyltransferases EZH2 and EZH1. ACS Chem Biol 2013;8:1324–34.
25. Xu B, On DM, Ma A, Parton T, Konze KD, Pattenden SG, et al. Selective inhibition of EZH2 and EZH1 enzymatic activity by a small molecule suppresses MLL-rearranged leukemia. Blood 2015;125:346–57.
26. McGrath J, Trojer P. Targeting histone lysine methylation in cancer. Pharmacol Ther 2015;150:1–22.
27. Huang Z, Wu H, Chuai S, Xu F, Yan F, Englund N, et al. NSD2 is recruited through its PHD domain to oncogenic gene loci to drive multiple myeloma. Cancer Res 2013;73:6277–88.
28. Luense S, Denner P, Fernandez-Montalvan A, Hartung I, Husemann M, Stresemann C, et al. Quantification of histone H3 Lys27 trimethylation (H3K27me3) by high-throughput microscopy enables cellular large-scale screening for small-molecule EZH2 inhibitors. J Biomol Screen 2015;20:190–201.
29. Richter GH, Plehm S, Fasan A, Rossler S, Unland R, Bennani-Baiti IM, et al. EZH2 is a mediator of EWS/FLI1 driven tumor growth and metastasis blocking endothelial and neuro-ectodermal differentiation. Proc Natl Acad Sci U S A 2009;106:5324–9.
30. Matsuo Y, Drexler HG, Harashima A, Okochi A, Hasegawa A, Kojima K, et al. Induction of CD28 on the new myeloma cell line MOLP-8 with t(11;14)(q13;q32) expressing delta/lambda type immunoglobulin. Leuk Res 2004;28:869–77.
31. Pawlyn C, Kaiser MF, Davies FE, Morgan GJ. Current and potential epigenetic targets in multiple myeloma. Epigenomics 2014;6:215–28.
32. Azab AK, Hu J, Quang P, Azab F, Pitsillides C, Awwad R, et al. Hypoxia promotes dissemination of multiple myeloma through acquisition of epithelial to mesenchymal transition-like features. Blood 2012;119: 5782–94.
33. Dimopoulos K, Gimsing P, Gronbaek K. The role of epigenetics in the biology of multiple myeloma. Blood Cancer J 2014;4:e207.
34. Morey L, Helin K. Polycomb group protein-mediated repression of transcription. Trends Biochem Sci 2010;35:323–32.
35. Sneeringer CJ, Scott MP, Kuntz KW, Knutson SK, Pollock RM, Richon VM, et al. Coordinated activities of wild-type plus mutant EZH2 drive tumor-associated hypertrimethylation of lysine 27 on histone H3 (H3K27) in human B-cell lymphomas. Proc Natl Acad Sci U S A 2010;107:20980–5.

36. Shen H, Laird PW. Interplay between the cancer genome and epigenome. Cell 2013;153:38–55.
37. Amatangelo MD, Garipov A, Li H, Conejo-Garcia JR, Speicher DW, Zhang R. Three-dimensional culture sensitizes epithelial ovarian cancer cells to EZH2 methyltransferase inhibition. Cell Cycle 2013;12: 2113–9.
38. Malouf GG, Taube JH, Lu Y, Roysarkar T, Panjarian S, Estecio MR, et al. Architecture of epigenetic reprogramming following Twist1-mediated epithelial-mesenchymal transition. Genome Biol 2013;14:R144.
39. Cao Q, Yu J, Dhanasekaran SM, Kim JH, Mani RS, Tomlins SA, et al. Repression of E-cadherin by the polycomb group protein EZH2 in cancer. Oncogene 2008;27:7274–84.
40. Parvani JG, Schiemann WP. Sox4, EMT programs, and the metastatic progression of breast cancers: mastering the masters of EMT. Breast Cancer Res 2013;15:R72.
41. Liu L, Xu Z, Zhong L, Wang H, Jiang S, Long Q, et al. Enhancer of zeste homolog 2 (EZH2) promotes tumour cell migration and invasion via epigenetic repression of E-cadherin in renal cell carcinoma. BJU Int. Epub 2014 Feb 25.
42. Wu Y, Zhang L, Zhang L, Wang Y, Li H, Ren X, et al. Long non-coding RNA HOTAIR promotes tumor cell invasion and metastasis by recruiting EZH2 and repressing E-cadherin in oral squamous cell carcinoma. Int J Oncol 2015;46:2586–94.
43. Zhang J, Cao W, Xu Q, Chen WT. The expression of EMP1 is downregulated in oral squamous cell carcinoma and possibly associated with tumour metastasis. J Clin Pathol 2011;64:25–9.
44. Sun GG, Wang YD, Cui DW, Cheng YJ, Hu WN. EMP1 regulates caspase-9 and VEGFC expression and suppresses prostate cancer cell proliferation and invasion. Tumour Biol 2014;35:3455–62.
45. Sun G, Zhao G, Lu Y, Wang Y, Yang C. Association of EMP1 with gastric carcinoma invasion, survival and prognosis. Int J Oncol 2014;45:1091–8.
46. Herath NI, Boyd AW. The role of Eph receptors and ephrin ligands in colorectal cancer. Int J Cancer 2010;126:2003–11.
47. Cortina C, Palomo-Ponce S, Iglesias M, Fernandez-Masip JL, Vivancos A, Whissell G, et al. EphB-ephrin-B interactions suppress colorectal cancer progression by compartmentalizing tumor cells. Nat Genet 2007; 39:1376–83.
48. Gadea G, Blangy A. Dock-family exchange factors in cell migration and disease. Eur J Cell Biol 2014;93:466–77.
49. Sassano A, Mavrommatis E, Arslan AD, Kroczynska B, Beauchamp EM, Khuon S, et al. Human schlafen 5 (SLFN5) is a regulator of motility and invasiveness of renal cell carcinoma cells. Mol Cell Biol 2015;35:2684–98.
50. Katsoulidis E, Mavrommatis E, Woodard J, Shields MA, Sassano A, Carayol N, et al. Role of interferon {alpha} (IFN{alpha})-inducible Schlafen-5 in regulation of anchorage-independent growth and invasion of malignant melanoma cells. J Biol Chem 2010;285:40333–41.